Measuring stratospheric H_2O with an airborne spectrometer: test with a realistic detector

Maziar Bani Shahabadi[1], Yi Huang[1], Louis M. Moreau[2]*

[1]Department of Atmospheric and Oceanic Science, McGill University, Montreal, QC, Canada

[2]ABB Inc., Quebec City, QC, Canada

Corresponding author: Maziar Bani Shahabadi, Department of Atmospheric and Oceanic Science, McGill University, Room 945, Burnside Hall, 805 Sherbrooke Street West, Montreal, Quebec, Canada, H3A 0B9. Email: maziar.banishahabadi@mail.mcgill.ca

Abstract

This study examines the ability of a realistic spectral sensor flying at the tropopause level for retrieving stratospheric H_2O. This paper is an extension of an earlier study; the assumptions to best fit the characteristics of the operational sensors have been updated. Several tests are conducted to examine the effects of changing spectral coverage and noise level on the quality of the stratospheric temperature and H_2O retrievals. Using the current technology, it is recommended to reduce the noise level by increasing the observation time one order of magnitude in order to have satisfactory retrievals. In the earlier study, we determined that including far InfraRed (IR) in the sensor's spectral coverage is essential for achieving accurate H_2O retrieval. However, the results here indicate that enabling the far IR at the cost of sacrificing mid IR sensitivity does not help to improve H_2O retrieval or temperature retrieval in realistic sensor. Such hyper-spectral instrument can achieve the retrieval accuracy of 0.5 ppmv for H_2O and 1 K for temperature up to 50 hPa. The potential of high sensitivity retrieval is advantageous for detecting the small temporal/spatial scale lower stratospheric moistening episodes.

1 Introduction

Stratospheric water vapor (H_2O) is an important contributor to climate system that cannot be neglected. It cools the stratosphere by emitting Outgoing Longwave Radiation (OLR) to outer space, but warms the troposphere by radiating InfraRed (IR) radiation downward to the surface. Although it may significantly affect the Earth radiation budget during climate change (Forster & Shine, 1999) (Solomon, et al., 2010), this effect is not well quantified, largely due to uncertainty in water vapor change in both climate models (Gettelman & Coauthors, 2010) and observations (Hegglin & Coauthors, 2013). This justifies the necessity of measuring the stratospheric H_2O with great accuracy. Satellite observations, using limb and occultation sounders such as SAGE II (Thomason, Burton, Iyer, Zawodny, & Anderson, 2004) HALOE (Russell & Coauthors, 1993) MLS/UARS (Livesey &

Coauthors, 2003), and ACE-FTS (Bernath & Coauthors, 2005), are sensitive to stratospheric H_2O but have large sampling footprints that make the detection of the small-scale water vapor variation a challenging task.

Compared to the satellites sounders, an airborne measurement has much smaller sampling footprint that can capture small-scale variability. Using an uplooking airborne spectrometer, deployed on an aircraft or a balloon flown below the stratosphere, was suggested by (Bani Shahabadi & Huang, 2014) (hereinafter BH14) for stratospheric H_2O measurement. This paper is an extension of this earlier conducted study with an update of our assumptions to best fit the characteristics of the operational detectors. The goal of this paper is to examine how well a realistic instrument can retrieve the stratospheric H_2O. Secondly, the different implementation strategies to improve the performance are investigated. In Section 2, the simulation and methodology are described. Results are presented in Section 3. Concluding remarks are given in Section 4.

2 Methodology

The same data/methods as BH14 is used in this study. The Gauss-Newton iteration method of the optimal estimation technique (Rodgers, 2000) is used and formulated as:

$$\hat{\mathbf{x}}_{\mathbf{i+1}} = \mathbf{x_0} + (\mathbf{K_i}^{\mathrm{T}}\mathbf{S_e}^{-1}\mathbf{K_i} + \mathbf{S_a}^{-1})^{-1}\mathbf{K_i}^{\mathrm{T}}\mathbf{S_e}^{-1}[\mathbf{y} - \mathrm{F}(\hat{\mathbf{x}}_{\mathbf{i}}) + \mathbf{K_i}(\hat{\mathbf{x}}_{\mathbf{i}} - \mathbf{x_0})] \quad (1)$$

which computes a new estimate for the state vector ($\hat{\mathbf{x}}_{\mathbf{i+1}}$) at each iteration i. $\mathbf{K_i}$ is the Jacobian at the current state vector estimate, $\mathbf{S_a}$ is the a priori covariance of the state vector and $\mathbf{S_e}$ is the covariance of the measurement error. $\mathrm{F}(\mathbf{x})$ is the forward model result, which is radiance. The indices $^{\mathbf{T}}$ and $^{\mathbf{-1}}$ are matrix transpose and inverse operators, respectively. The iteration proceeds until convergence or the maximum number of iteration reaches (10). The convergence criteria follow BH14.

The forward model is the Line-By-Line Radiative Transfer Model (LBLRTM, version 12.2)

from Atmospheric and Environmental Research (AER) (Clough, Iacono, & Moncet, 1992) (Clough, et al., 2005). The atmospheric temperature and water vapor at 12 fixed pressure levels (10 hPa-spaced between 100 and 10 hPa, and then 5 hPa, and 1 hPa) are considered for the retrieval test. For line-by-line molecular absorption, Voigt profile is considered and all the H_2O continua are considered. No aerosol or solar input at the top-of-the-atmosphere (TOA) is considered. The LBLRTM model calculates the emission spectrum, ignoring the scattering processes. Six molecular species are included in the calculation, namely H_2O, CO_2, O_3, N_2O, CO, and CH_4, which are active gas species in the infrared region.

Stratospheric temperature and H_2O profiles were obtained from the ACE-FTS instrument (Bernath & Coauthors, 2005). Only the North American profiles (30°N < latitude < 60°N and 70°W < longitude < 130°W, between years 2004-2009) are selected for retrieval test. ACE-FTS is a solar occultation instrument covering a spectral range from 750 to 4400 cm^{-1} with a spectral sampling interval of 0.02 cm^{-1}. The satellite instrument samples atmospheric volumes that stretch a few kilometers vertically and hundreds of kilometers horizontally (Bernath & Coauthors, 2005), therefore it does not capture smaller scale atmospheric variability. To enhance the H_2O concentration variability in the dataset, we artificially moistened the H_2O profiles to a randomly-selected 20 hPa thick segment of the profile. It was checked that the moistening prescribed here is very modest compared to the magnitude measured by (Anderson, Wilmouth, Smith, & Sayres, 2012). The mean of profiles is used as the a priori (first guess) in the retrieval tests. Figure 4 in BH14 shows the correlation matrix of the dataset.

In the retrieval equation (Eq (1)), the sensor is assumed to have spectrally uncorrelated noise (noise covariance matrix is a diagonal matrix). In BH14, the results were developed based on uniform noise magnitude across the entire spectrum and the noise-equivalent delta radiance (NEDR) was altered between 0.25×10^{-7} W cm^{-2} sr^{-1} cm and 0.75×10^{-7} W cm^{-2} sr^{-1} cm, representing low and high noise

levels, respectively. These two noise levels were chosen in BH14 to envelop the instrument noise level in the Climate Absolute Radiance and REfractivity Observatory (CLARREO) instrument (Mlynczak, 2010) (Wielicki & Coauthors, 2013). However, the NEDR of realistic spectrometer will be a combination of the low noise level at the mid IR spectral region (650 to 2000 cm^{-1}) and the high noise level at the far IR (200 to 650 cm^{-1}) region (Merrelli & Turner, 2012). The NEDR values used in this study are estimated with an in-house mathematical model based on real ABB spectrometer. The input to the model was based on the interferometer sizing and performance (optics, field of view, resolution, etc.) that ABB built for GOSAT (Moreau & Coauthors, 2009) (Moreau, Veilleux, & Suto, 2014). The sampling interval is 0.2 cm^{-1}, observation time is 1 s, with Field Of View (FOV) of 15.8 mrad for this instrument. Two spectrally variable NEDR values are implemented in different retrieval tests in this study: 1) One NEDR spectrum is based on a typical cooled detector with cutoff near 700 cm^{-1} for mid IR and a typical uncooled pyro-electrical detector for the far IR. Since the instrument has and agreeable performance in mid IR, i.e. low NEDR values, its NEDR is referred to as MIR, henceforth; 2) One NEDR spectrum is based on a commercial cooled detector with cut-off near 435 cm^{-1} and a typical uncooled pyro-electrical detector for the far IR (< 435 cm^{-1}). Compared to the first instrument, it has the same NEDR below 435 cm^{-1}, and it has a lower noise from 435-700 cm^{-1} at the price of reduced performance beyond 700 cm^{-1}. This NEDR is referred to as FIR. The FIR/MIR NEDR spectrums are compared to low/high noise levels in BH14 in Figure 1.

All of the line by line calculations of radiance and Jacobian are performed with a monochromatic resolution of 0.001 cm^{-1}. Then they are convolved with sinc spectral response function to spectral resolutions with desired Half-Width Half-Maximum (HWHM). The convolved radiance and Jacobian are used as input in the retrieval algorithm. Spectral Jacobian for H_2O ($\mathbf{K_q}$) and temperature ($\mathbf{K_T}$) are shown in Figure 6 in BH14. Different spectral intervals between 200-2000 cm^{-1} are investigated here and the merit of each spectral interval for the retrieval of temperature and H_2O is

examined and compared.

Same as in BH14, the quality of the retrieval is determined by comparing 1) the Root Mean Square (RMS) of the differences between the retrieved and truth quantities at each level for all of the test profiles; 2) the standard deviation (STD) of the dataset.

3 Sounding of stratospheric Temperature/H_2O

3.1 FIR vs. MIR noise performance

We examine how precisely the iteration technique can reproduce the truth profile in two different scenario of using FIR and MIR noise spectrum. We limit our retrieval tests to the unmoistened original ACE-FTS profiles for now.

For information content assessment, the Degrees of Freedom for Signal (DFS) is used, similar to BH14 and other former studies (Worden & Coauthors, 2004) (Merrelli & Turner, 2012). DFS is defined as the trace of averaging kernel matrix, following (Rodgers, 2000), and formulated as:

$$\mathbf{A} = (\mathbf{K_i}^T \mathbf{S_e}^{-1} \mathbf{K_i} + \mathbf{S_a}^{-1})^{-1} \mathbf{K_i}^T \mathbf{S_e}^{-1} \mathbf{K_i} \quad (4)$$

The NEDR is inversely proportional with resolution, the square root of the observation time, and the square of the aperture diameter. For instance to gain 10 times noise reduction, the observation time and the aperture diameter could be increased simultaneously by 10 and $10^{0.25}$ times, respectively. Keeping the spectral resolution fixed, the impact of noise reduction due to the combined increase in observation time/aperture diameter on temperature and H_2O DFS is shown in Figure 2. The results show that, using both FIR/MIR noise spectrums to detect a single piece of information about stratospheric H_2O (H_2O DFS equal to one), one needs to have an order of magnitude noise reduction. This implies that satisfactory stratospheric H_2O retrieval performance is not achievable, unless the

126 NEDR spectrum is reduced, at least 10 times. MIR noise spectrum captures more pieces of information
127 (potential of better retrieval) about stratospheric temperature, compared to that of FIR noise. Also
128 having the far IR spectral interval and MIR noise spectrum, the sensor has the best prospect of less
129 erroneous stratospheric H_2O retrieval.

130 Figure *3* shows the averaging kernel for temperature and H_2O using 10 times noise reduction
131 factor (spectral range = 700-2000 cm^{-1}, resolution = 0.2 cm^{-1}, observation time = 10 s, increase in
132 aperture diameter by $10^{0.25} \sim 12$ cm, noise = MIR). The rows of averaging kernel matrix act to smooth
133 the retrieved state estimated error at each level (Rodgers, 2000), and the FWHM of the linearly
134 interpolated kernel represent of the vertical resolution as function of altitude in the retrieval results
135 (Merrelli & Turner, 2012). The rows 2, 5, 7, and 10 (out of 12), corresponding to different pressure
136 levels, of the averaging kernels are shown here. The total DFS is 1.4, and 5.4 for H_2O, and temperature,
137 respectively. The Cumulative DFS normalized by the Total DFS (Figure *3*, panel (c)) shows that 100-
138 60hPa and 100-10hPa vertical segments contain 80% of the information for H_2O and temperature,
139 respectively.

140 Numerous tests are conducted to examine the effects of changing spectral coverage, and noise
141 level on the quality of the retrievals. Table 1 outlines the experiment cases that are investigated. Case 1
142 represents the reference sensor setting. Case 2 examines the impact of sacrificing the mid IR
143 performance for low noise (FIR) measurements in 435-700 cm^{-1} spectral range. Compared to Case 1,
144 the RMS error in temperature retrieval increases and there is no significant change in H_2O retrieval
145 performance. Both of temperature/H_2O information contents (DFS) decrease. This means higher FIR
146 noise levels, beyond 700 cm^{-1}, act to deteriorate the temperature retrieval. Knowing that ozone band
147 has large sensitivity to temperature (Figure 6 in BH14), higher noise levels spoil the use of these
148 channels for temperature retrieval. Compared to Case 2, Case 3 indicates the added value of including
149 200-435 cm^{-1} spectral range in temperature/H_2O retrievals. As seen, including the 200-435 cm^{-1}

150 spectral band does not help to improve the retrievals and no extra temperature/H_2O information is
151 added. Compare to Case 1, Case 4 determines the impact of adding noisy measurement of 200-700 cm^{-1}
152 band. Although, the DFS results show the added information about H_2O, but due to higher noise in far
153 IR, the retrieval algorithm cannot use the added information to improve the H_2O retrieval performance
154 and lower the RMS error, compared to Case 1. Case 5 represents the impact of lowering the spectral
155 resolution to 1 cm^{-1}. There is added information for both temperature and H_2O, compared to Case 1.
156 The retrieval RMS results (figure not shown) indicates that Case 5 has the same performance as Case 1
157 in terms of H_2O retrieval, while Case 1 does a slightly better temperature retrieval in lower to mid
158 stratosphere. Since Case 5 has an agreeable performance for both H_2O and temperature retrievals,
159 considering its smaller interferometer size and easier onboard installation, we recommend Case 5
160 among the test cases mentioned above. We find that this hyperspectrometer with a 700-2000 cm^{-1}
161 spectral coverage, a 1 cm^{-1} spectral sampling interval, and a MIR noise level can generally achieve a
162 retrieval accuracy of 0.4 ppmv for H_2O and 1 K for temperature up to about 50 hPa.
163 The above results will change depending on the noise reduction factor (only observation time
164 here) implemented. The current technology can detect event as small as sampled in approximate 10 s
165 observation time of the instrument, which differs greatly among the platforms (e.g., jetliner (1000
166 km/hr) – 2.8 km; balloon (drifted by 10 m/s wind) – 100 m). BH14 reported that far IR (using constant
167 noise level throughout the spectrum) might benefit stratospheric H_2O retrieval. However, given the
168 noise performance of the detectors analyzed here, including FIR does not improve H_2O retrieval.
169 Instead, satisfactory retrieval can be achieved by collectively increasing the stare-time at the target and
170 aperture diameter, which effectively reduces the detector noise. This strategy can be best realized by
171 flying the instrument on airship, air balloon or hovering aircraft.
172

3.2 Detection of moistening

Same as BH14, we test how well the stratospheric moistening episodes as identified by (Anderson, Wilmouth, Smith, & Sayres, 2012) are captured using the recommended sensor (Case 5 in Table 1). We include the profiles that are artificially moistened together with the unmoistened profiles in the retrieval algorithm. The RMS errors in the retrieval of truth profiles with and without moistened profiles are shown in Figure 4. Although the RMS error in the moistened case is larger than the unmoistened case, it is considerably less compared to the uncertainty in the a priori guess. In general, more than 50% reduction in the uncertainty is attained for the vertical distribution of H_2O. The retrieval accuracy is better than 0.5 ppmv for H_2O and 1 K for temperature up to 50 hPa. The RMS of the fractional error between the retrieved and truth H_2O loadings is 1.2% (unmoistened: 1%; moistened: 1.4%). The results show that the retrieval algorithm can well capture the H_2O concentration in both dry and moist cases.

4 Conclusion

Stratospheric H_2O is an important factor that affects climate change. Airborne spectrometers have shown to be useful observational tools that may supplement existing in situ and satellite observations. This study is an extension to (Bani Shahabadi & Huang, 2014) and examines the feasibility of the realistic spectrometers flying at tropopause level to observe stratospheric H_2O.

Observational data derived from the ACE-FTS satellite are used for testing the instrument performance. Synthetic downwelling radiance is obtained by the LBLRTM radiation code. Gauss-Newton iterative technique is used to obtain a solution from the retrieval algorithm. This study shows that a realistic spectrometer, with 700-2000 cm^{-1} spectral coverage, 1 cm^{-1} spectral resolution, 10 s observation time, and 12 cm aperture diameter is able to reach the retrieval accuracy of 0.4 ppmv and 1

K for simultaneous retrieving H_2O and temperature in the lower to middle stratosphere. Therefore, the current operational sensors with these specifications, including Scanning High-resolution Interferometer Sounder (S-HIS) (Revercomb & Coauthors, 1998) and Atmospheric Emitted Radiance Interferometer (AERI) (Demirgian & Dedecker, 2005), can be utilized for agreeable stratospheric H_2O retrieval with minimal modifications. The results show the retrievals become unreliable above 10 hPa and 40 hPa, respectively, for temperature and the H_2O. The results indicate that using the current technology, enabling the far IR measurement in detectors, that comes with the cost of sacrificing mid IR noise performance, does not help to improve H_2O retrieval or temperature retrieval.

Using an airborne spectrometer with a fast response time provides the opportunity to monitor lower stratospheric moistening events (Anderson, Wilmouth, Smith, & Sayres, 2012). This study confirms that the current sensor can achieve the retrieval accuracy of 0.5 ppmv for H_2O and 1 K for temperature up to 50 hPa to detect the small temporal/spatial scale moistening episodes.

Acknowledgment

This work is supported by the NSERC Discovery Program. We thank ABB Inc. personnel, Mr. Louis M. Moreau and Dr. Richard L. Lachance, for providing the NEDR data.

References

Anderson, J. G., Wilmouth, D. M., Smith, J. B., & Sayres, D. S. (2012). UV dosage levels in summer: Increased risk of ozone loss from convectively injected water vapor. *Science , 337*, 835– 839.

Bani Shahabadi, M., & Huang, Y. (2014). Measuring Stratospheric H2O with an Airborne Spectrometer. *J. Atmos. Oceanic Technol. , 31*, 1502-1515.

Bernath, P. F., & Coauthors. (2005). Atmospheric Chemistry Experiment (ACE): Mission overview. *Geophys. Res. Lett. , 32*, L15S01.

Clough, S., Iacono, M., & Moncet, J. (1992). Line-by-line calculations of atmospheric fluxes and cooling rates: Application to water vapor. *J. Geophys. Res. , 97*, 15761-15785.

Clough, S., Shephard, M., Mlawer, E., Delamere, J., Iacono, M., Cady-Pereira, K., et al. (2005). Atmospheric radiative transfer modeling: a summary of the AER codes . *J. Quant. Spectrosc. Radiat. Transfer , 91*, 233-244 .

Demirgian, J., & Dedecker, R. (2005). *Atmospheric Emitted Radiance Interferometer (AERI) Handbook.* Atmospheric Radiation Measurement (ARM), U.S. Department of Energy.

Forster, P. M., & Shine, K. P. (1999). Stratospheric water vapour changes as a possible contributor to observed stratospheric cooling. *Geophys. Res. Lett. , 26*, 3309–3312.

Gettelman, A., & Coauthors. (2010). Multimodel assessment of the upper troposphere and lower stratosphere: Tropics and global trends. *J. Geophys. Res. , 115*, D00M08.

Hegglin, M. I., & Coauthors. (2013). SPARC Data Initiative: Comparison of water vapor climatologies from international satellite limb sounders. *J. Geophys. Res. , 118*, 11824–11846.

Livesey, N. J., & Coauthors. (2003). The UARS Microwave Limb Sounder version 5 data set: Theory, characterization, and validation. *J. Geophys. Res. , 108*, 4378.

Merrelli, A., & Turner, D. D. (2012). Comparing information content of upwelling far-infrared and midinfrared radiance spectra for clear atmosphere profiling. *J. Atmos. Oceanic Technol. , 29*, 510–526.

Mlynczak, M. G. (2010). *Infrared instrument overview.* Retrieved from http://clarreo.larc.nasa.gov/workshops/2010STM/ Wednesday/IR_Final_Mlynczak.pptx

Moreau, L. M., & Coauthors. (2009). Overview of the Test Activities Performed on the Interferometer of GOSAT / TANSO-FTS, Fourier Transform Spectroscopy. *OSA Technical Digest Series.* Vancouver.

Moreau, L. M., Veilleux, J., & Suto, H. (2014). The GOSAT / TANSO interferometer after five years on orbit, Infrared Instruments I. *SPIE.* San Diego.

Oltmans, S. J., Vomel, H., Hofmann, D. J., Rosenlof, K. H., & Kley, D. (2000). The increase in stratospheric water vapor from balloonborne, frostpoint hygrometer measurements at Washington, D.C., and Boulder, Colorado. *Geophys. Res. Lett. , 27*, 3453–3456.

Revercomb, H. E., & Coauthors. (1998). Recent results from two new aircraft-based Fourier-transform interferometers: The Scanning High-Resolution Interferometer Sounder and the NPOESS Atmospheric Sounder Testbed Interferometer. *Proc. Eighth Int. Workshop on Atmospheric Science from Space Using Fourier Transform Spectrometry.* Toulouse, France.

Rodgers, C. D. (2000). *Inverse Methods for Atmospheric Sounding: Theory and Practice. Series on Atmospheric, Oceanic and Planetary Physics,.* World Scientific Publishing.

Russell, J. M., & Coauthors. (1993). The Halogen Occulation Experiment. *J. Geophys. Res. , 98*, 10777–10797.

Solomon, S., Rosenlof, K. H., Portmann, R. W., Daniel, J. S., Davis, S. M., Sanford, T. J., et al. (2010). Contributions of stratospheric water vapor to decadal changes in the rate of global warming. *Science , 327*, 1219–1223.

Thomason, L. W., Burton, S. P., Iyer, N., Zawodny, J. M., & Anderson, J. (2004). A revised water vapor product for the Stratospheric Aerosol and Gas Experiment (SAGE) II version 6.2 data set. *J. Geophys. Res. , 109*, D06312.

Wielicki, B. A., & Coauthors. (2013). Achieving climate change absolute accuracy in orbit. *Bull. Amer.*

Meteor. Soc. , 94, 1519– 1539.

Worden, J., & Coauthors. (2004). Predicted errors of tropospheric emission spectrometer nadir retrievals from spectral window selection. *J. Geophys. Res. , 109*, D09308.

Tables

Table 1. Different test scenarios. Observation time = 10 s and aperture diameter = 12 cm to achieve 10 times noise reduction factor for all cases.

RMS	Spectral Sampling (cm^{-1})	Spectral Range (cm^{-1})	Noise (W cm^{-2} sr^{-1} cm)	DFS T/q
Case 1	0.2	700-2000	MIR	5.45/1.27
Case 2	0.2	435-2000	FIR	3.99/1.14
Case 3	0.2	200-2000	FIR	3.99/1.29
Case 4	0.2	200-2000	MIR	5.44/1.39
Case 5	1	700-2000	MIR	5.75/1.36

Figures

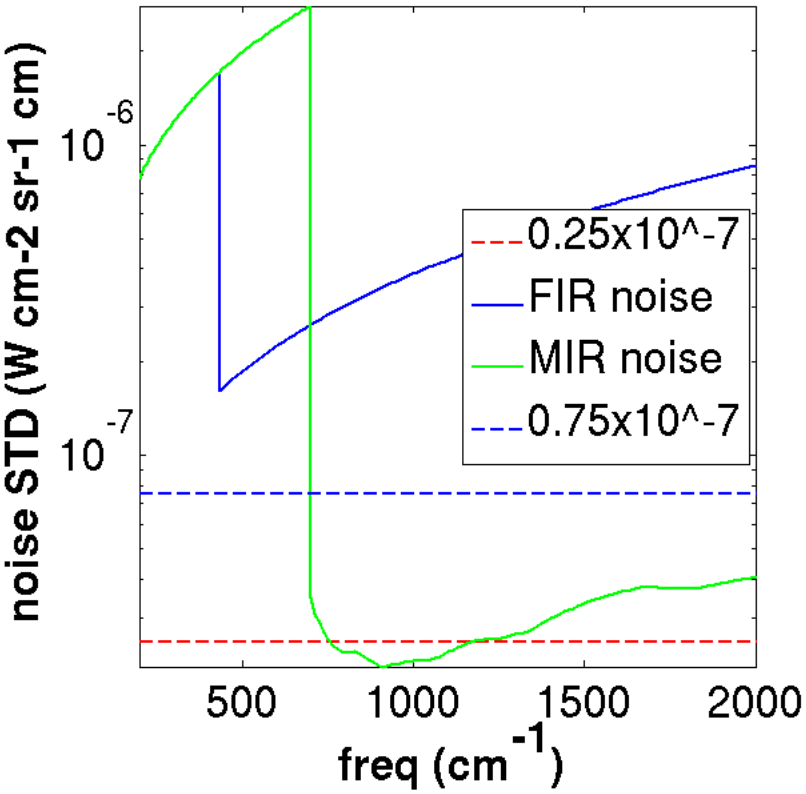

Figure 1. Comparison of FIR/MIR NEDR obtained from ABB Inc (solid lines), and previously used (dashed lines)NEDR spectrum in BH14.

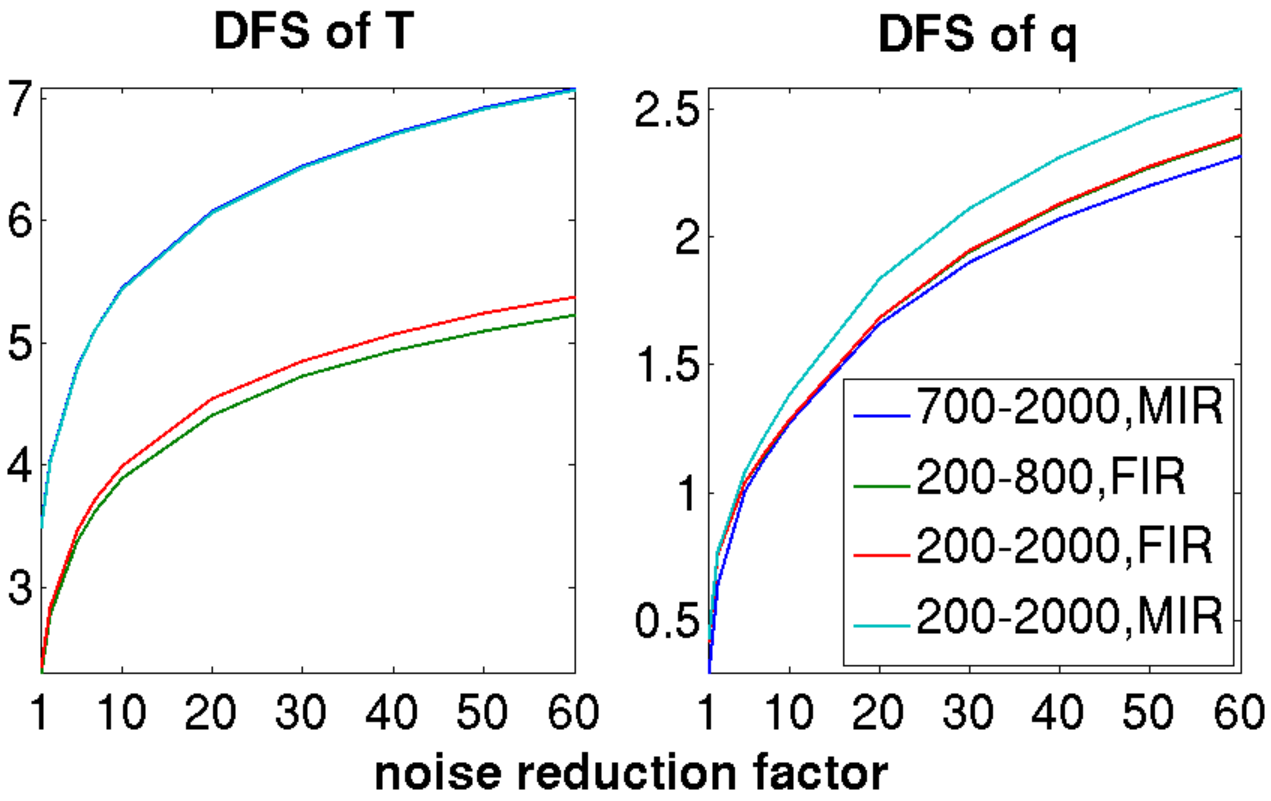

Figure 2. Temparature/H_2O DFS change with noise reduction factor for different spectral intervals. Spectral resolution is 0.2 cm^{-1} for all test cases.

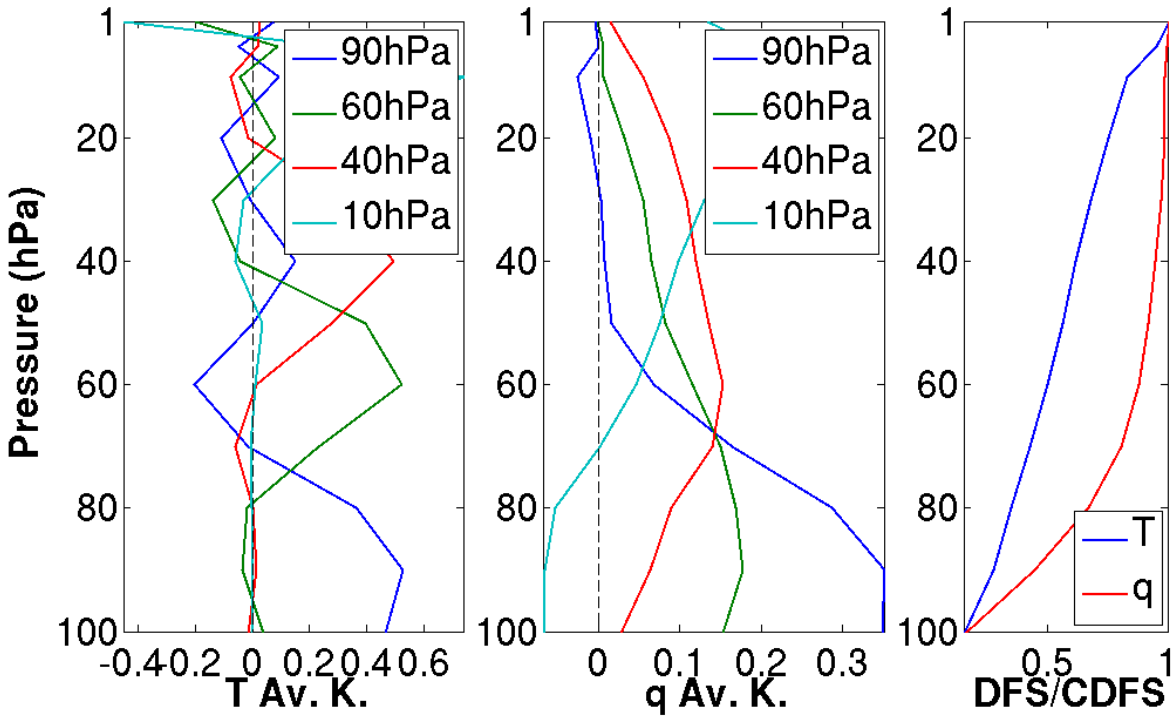

Figure 3. *Temperature/H_2O averaging kernel and DFS (spectral range = 700-2000 $cm^{-}1$, resolution = 0.2 cm^{-1}, observation time = 10 s, noise = MIR)*

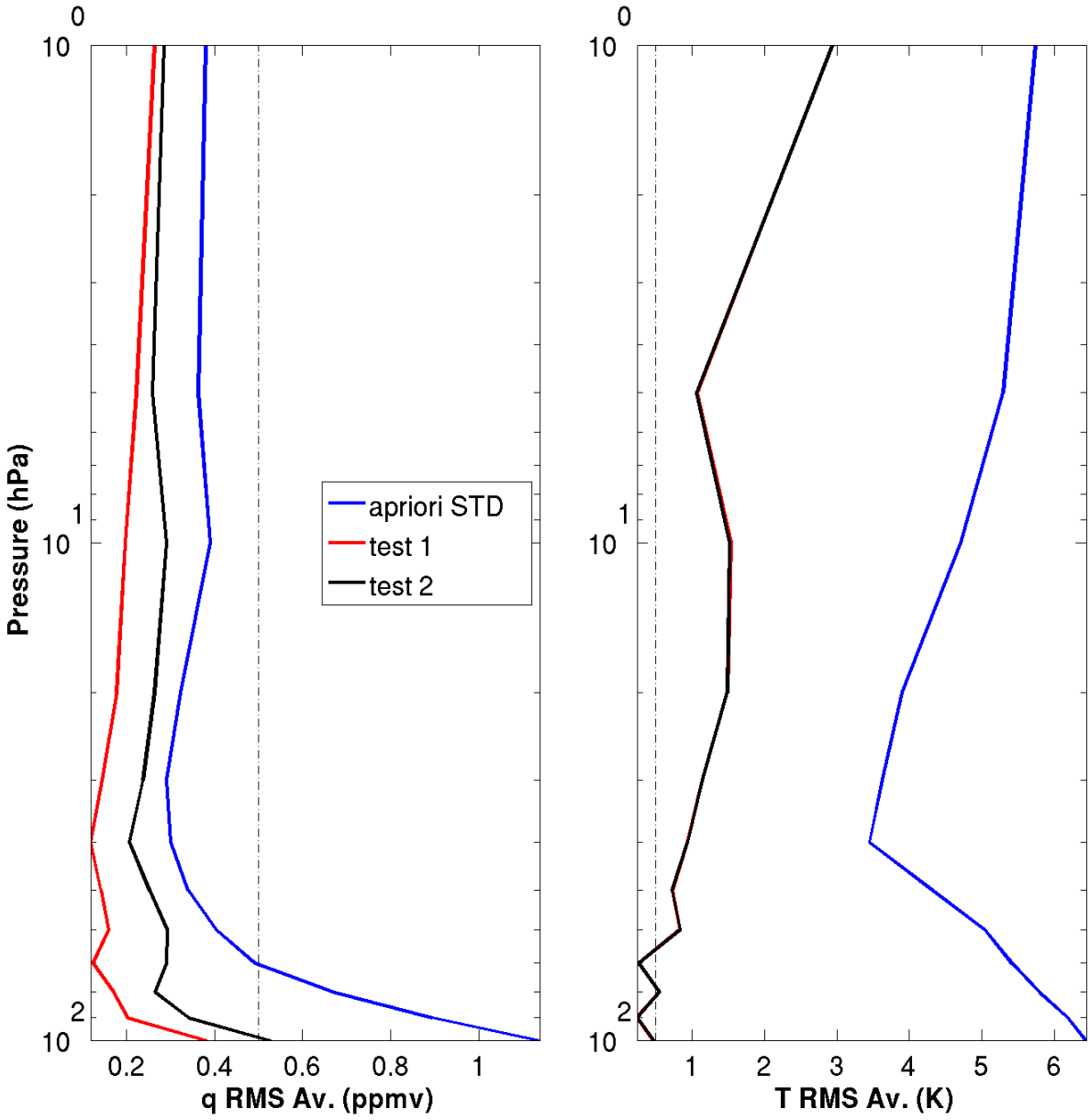

Figure 4. Ability of reference sensor (Case 5 in Table 1) to retrieve dry and moistened profiles. test 1: RMS of dry profiles retrievals, and test 2: RMS of moistened profiles retrievals.